Vietnam Journal of Science and Technology ***61*** *(1) (2023) 1-26*

doi:10.15625/2525-2518/17666

Review: Emulsion techniques for producing polymer based drug delivery systems

Nguyen Thuy Chinh[1, 2], Thai Hoang[1, 2, *]

[1]*Institute for Tropical Technology, Vietnam Academy of Science and Technology, 18 Hoang Quoc Viet, Cau Giay, Ha Noi, Viet Nam*

[2]*Graduate University of Science and Technology, Vietnam Academy of Science and Technology, 18 Hoang Quoc Viet, Cau Giay, Ha Noi, Viet Nam*

[*]Email: *hoangth@itt.vast.vn*

Received: 19 November 2022; Accepted for publication: 13 January 2023

Abstract. Emulsification method is one of the popular methods for producing materials used in biosensing, bioimaging and others, especially, drug delivery polymer systems in microsize and nanosize. The concrete techniques related to this method are emulsification, self-emulsification, in a combination with solvent evaporation process, homogenization, or ultranosication. The structure of emulsion formulation consists of two phases: an internal phase and an external phase. Based on the structure and nature of the phases, emulsions can be classified into different types such as two-phase systems (oil in water emulsion (O/W) or water in oil emulsion (W/O)) or three-phase systems (water in oil in water triple emulsion (W/O/W) or oil in water in oil triple emulsion (O/W/O)). The droplet sizes in micro-emulsion systems are often higher than 1 μm while those in nano-emulsions or mini-emulsions are in the range of 100 - 500 nm. Some special nano-emulsion systems can contain droplets with a size of few nanometers. Factors including solvents, oil/water phase ratio, droplet oil size, composition ratio, nature of raw materials, emulsifiers, etc. can affect the morphology, properties, and size of the obtained products. This paper reviews emulsion techniques which have been applied for producing polymeric drug delivery systems. The components, properties, characteristics, encapsulation efficiency as well as drug release rate, water solubility, toxicity and administration efficacy of drug emulsion formulations will be mentioned. Advantages and limitations of emulsion techniques are also discussed.

Keywords: Emulsion techniques, emulsification method, natural polymers, biopolymers, drug delivery.

Classification numbers: 2.3.1, 2.9.3, 2.10.2.

1. INTRODUCTION

Emulsion is known as a heterogeneous system containing very small liquid particles (ca. from several nanometers to tens of micrometers) dispersed in another liquid, in which the two liquids are insoluble. The definition of emulsion by the IUPAC states: “In an emulsion, liquid droplets and/or liquid crystals are dispersed in a liquid” [1]. An emulsion system usually

contains three main components including aqueous phase (polar liquid containing solutes dissolved in it), oily phase (nonpolar liquid containing solutes dissolved in it), and emulsifier (to support the formation of emulsions and stabilize emulsions). Emulsification method is applied to prepare emulsion systems containing two or three phases. In the presence of an emulsifier, it is easier to mix the oily phase and the aqueous phase to form a homogeneous emulsion system. Emulsions can be divided into macroemulsions, microemulsions, nano-emulsions (or mini-emulsions or submicron emulsions or ultrafine emulsions), multiple emulsions, etc. depending on the size of liquid droplets.

Up to now, microemulsions have become popular and are increasing dramatically in many fields of application thanks to their advantages such as thermodynamic stability as well as size control of the products [2]. Hoar and Schulman were the first to introduce the notion of microemulsions [3]. They used a medium chain length alcohol as an ionic surfactant to stabilize coarse macroemulsions. Schulman *et al.* suggested the word "microemulsion" in 1959 [4].

Microemulsions are different from nano-emulsions or micelles. Microemulsions are equilibrium systems while nano-emulsions are non-equilibrium systems, which tend to separate into the constituent phases and are kinetically stable [5]. Micelles have a core-shell structure with the core that can be added by chemical conjugation or physical entrapment [6].

In the biomedical field, emulsification technology is one of the popular pharmaceutical strategies that have been applied to enhance the bioavailability of chemical entities and active substances in general and of poorly water-soluble drugs in general. Microemulsions are the most popular emulsions due to their high thermodynamical stability and low viscosity, easy preparation and suitability for the preparation of polymer based drug delivery systems. They act as super-solvents for both water- and oil-soluble drugs. The drug microencapsulation or microparticles are prepared by emulsification method using a system containing ternary components, including polymer, drug and solvent (or solvent mixture) or by microemulsion method using W/O, O/W, W/O/W, or O/W/O systems. The emulsions have been reported to improve the bioavailability of peptide and protein drugs, anti-HIV drugs, and anti-cancer drugs [7 - 12].

The drug delivery microemulsion systems also have a long-lasting effect, thus reducing the total drug dose and minimizing the side effects of the drug. However, some limitations of microemulsions in the pharmaceutical field are that surfactants or co-surfactants are required to be safe, biocompatible, and pharmacologically acceptable; the drug loading capacity can be limited due to the high molecular weight of the drug; the long-term stability of the microemulsions may be influenced by the evaporation of solvent or the removal of the surfactants/co-surfactants.

2. EMULSION FORMATION CONDITIONS

A quantitative theory for describing the mechanism of emulsion formation is the thermodynamic treatment theory [13]. Accordingly, to form an emulsion system, it is necesscary to divide the dispersed phase into smaller liquid droplets. The energy required to disperse the liquid droplets transforms to Gibbs free energy on a specific surface in the emulsion (G). If the value of G is lower, the emulsion is more stable. G value could be calculated by the following equation:

$$G = \sigma S \quad (1)$$

where σ is the interface tension and S is total specific surface in the system.

One factor to evaluate the stability of emulsions is the delamination rate (v) that is calculated according to Stock equation:

$$v = \frac{2\,(d-d_0)gr^2}{9\eta} \quad (2)$$

where d and d_0 are the density of the dispersed phase and the dispersion medium, respectively; g is the gravity acceleration; r is the radius of the dispersed particles; η is the viscosity of the dispersion medium.

Some solutions applied to reduce G and v values include the use of surfactants or emulsifiers or the use of solvents/solutes with a suitable solubility in the internal and external phases to limit the change between d and d_0. Other factors that cause an increase in the viscosity of an emulsion include the viscosity of the internal and external phases, the chemical composition and polarity of the external phase, the droplet size and droplet size distribution of the dispersed phase, the natural volume and ratio of the substances in the internal phase, the composition, concentration and solubility of the emulsifier in the internal and external phases, the viscoelastic effect, and the presence of electrolytes, etc.

3. COMPOSITION OF EMULSIONS

The components of emulsion formulations for drug delivery often consist of main ingredients (oil, water, polymer and drug) and additional composition (for example, emulsifier, surfactant, co-surfactant). It is challenging to choose the ingredients for combination in the preparation of emulsions as well as the ratio of oil/water, concentration of polymer and drug in the medium, content of emulsifier, surfactant, etc. For a polymeric drug delivery, it is necessary to choose suitable components because the products will have to meet the biocompatibility and safety requirements.

Emulsions include two phases: dispersed phase or internal phase and medium phase or external phase. Phases may be aqueous phase, oily phase and emulsifier. If an emulsion is made up of an aqueous phase on the outside and an oily phase on the inside, it is called an oil-in-water emulsion. If an emulsion is made from an oily phase on the outside and an aqueous phase on the inside, it is called a water-in-oil emulsion (Figure 1). These are two commonly encountered microstructures of emulsions [14]. Besides, the bicontinuous microstructure is also a form of emulsion [15].

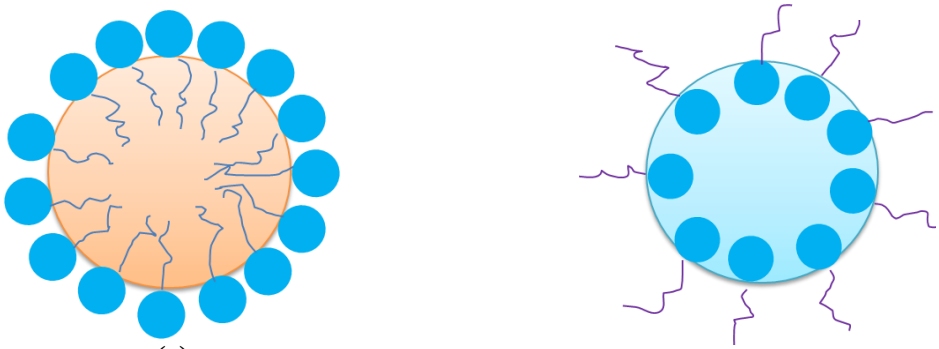

(a) (b)

Figure 1. Common microstructures of emulsion: Aqueous phase on the outside (a) and oily phase on the outside (b).

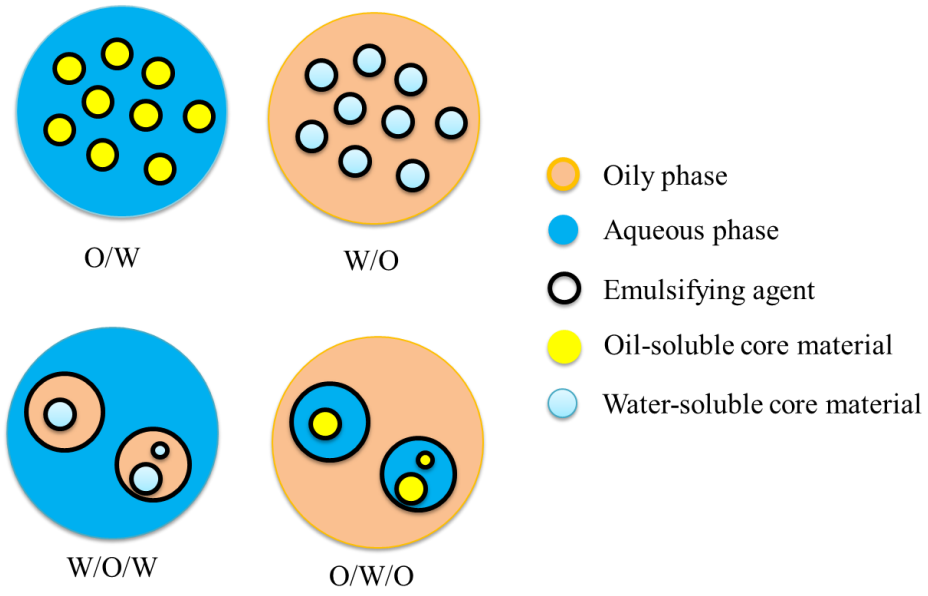

Figure 2. Typical types of emulsion formulations.

Typical types of emulsion formulations are shown in Figure 2. The water in oil (W/O) emulsion consists of oily phase, emulsifysing agent and water-soluble core material. The oil in water (O/W) emulsion is formed from aqueous phase, emulsifysing agent and oil-soluble core material. The water in oil in water (W/O/W) emulsion contains aqueous phase, oily phase and water-soluble core material. The oil in water in oil (O/W/O) emulsion includes oily phase, aqueous phase and oil-soluble core material.

Oily phase is a very important part of an emulsion system because it can affect the selection of other ingredients as well as the weight of dissolved lipophilic drugs, which influences the drug absorption from the gastrointestinal (GI) tract. The most suitable oily phase can completely dissolve the drugs. The common oils used for the preparation of emulsions are corn oil, olive oil, soyabean oil, peanut oil, sesame oil, oleic acid, ethyl oleate, propylene glycol dicaprylic ester, medium chain triglycerides (MCTs) and so on. The oils with long hydrocarbon chains, such as soybean oil, can dissolve a large content of lipophilic moieties but are difficult to microemulsify. The oils with shorter hydrocarbon chains, MCTs for example, are easier to microemulsify. Meanwhile, a mixed oil can be used for an emulsion system to reach the maximal solubility of the drug and facilitate the formation of this system. MCTs are one of the widely used oils for the preparation of emulsions because they are food grade products that are safe, stable and easy to form emulsions at ambient temperature.

In an emulsion system, the emulsifier is a key ingredient in the preparation of the emulsion. Emulsifiers may be surfactants, polymer emulsifiers, emulsifiers in the form of fine powders or emulsifiers generated instantaneously when combining two phases. The mechanism of action of an emulsifier is as follows: The emulsifier concentrates on the two-phase contact surface to form a protective coating for the dispersed particles. This coating has a high mechanical strength, is friendly to a dispersion medium and can be charged. This is to disperse the particles into the medium and stabilize the aggregate state of the particles. This mechanism can be applied for surfactants, however, the surfactants may also have a role in reducing the interface tension. The emulsifiers in the form of fine powders work according to the above mechanism while the

polymer emulsifiers work following the same mechanism and increase the viscosity of substances. The emulsifier type can be determined by a hydrophilic/lipophilic balance (HLB) index. The HLB index also helps to choose suitable surfactants for microemulsions. O/W emulsifying agents have HLB in the range of 8-16 while W/O emulsifying agents have HLB from 3 to 6 [16]. Some common emulsifiers are polysorbate 20, polysorbate 80, sorbitan monooleate, polyethylene glycol, glycerin, polyethylene oxide, lecithin, etc. Non-ionic emulsifiers are acceptable in pharmaceuticals [2].

The properties of the oil and emulsifier together with the oil/water ratio determine the tendency to form W/O or O/W microemulsions.

Drugs in emulsions may be water-soluble or poorly water-soluble. The distribution of hydrophobic drugs in W/O emulsions is less than that in O/W emulsions. The distribution of hydrophobic drug in an O/W emulsion is presented in Figure 3. The drug could be absorbed on the surface of the microemulsion (Figure 3a) or distributed together with the emulsifier near the surface of the microemulsion (Figure 3b) or concentrated in the interior of the microemulsion (Figure 3c).

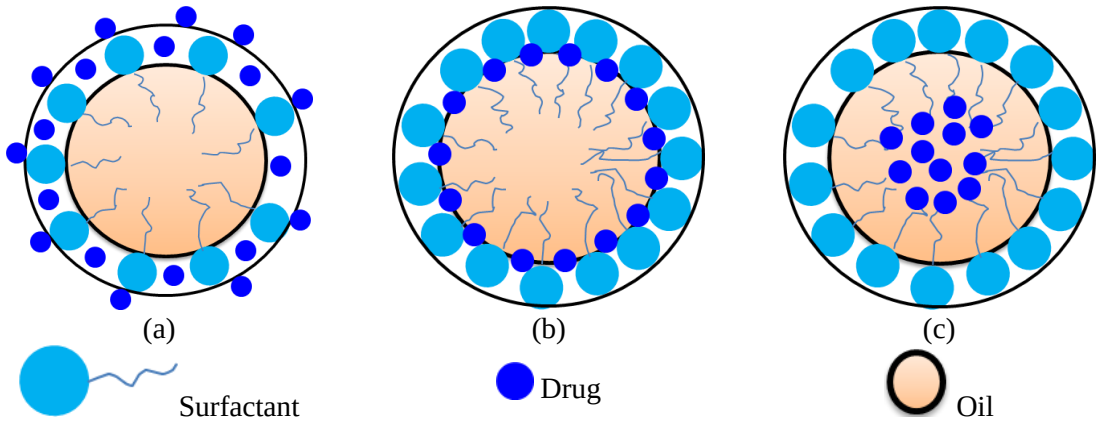

Figure 3. The hypothesized drug distribution in a microemulsion system. (a) microemulsion surface, (b) microemulsion interior, (c) palisade layer.

To increase the solubility and bioavailability of a poorly soluble drug, self-emulsifying systems (SES) have been applied for drug delivery. A self-emulsifying drug delivery system (SEDDS) is an isotropic mixture of oil, surfactant, and co-solvent [17], which can be used for oral delivery to enhance the absorption of drugs in intestinal. SEDDS can be divided into two types: self-microemulsifying drug delivery system (SMEDDS) and self-nanoemulsifying drug delivery system (SNEDDS) [18]. Most of the new drugs have low solubility in water, therefore, SEDDS is a potential candidate for forming new drug delivery systems [19, 20].

4. PREPARATION METHODS AND CHARACTERIZATION OF EMULSIONS

Based on the type of emulsion, the nature of ingredients and the desired product, a suitable method for the preparation of emulsion can be chosen. Because microemulsions have high thermodynamic stability, internal phase and external phase can be blended with the assistance of magnetic stirrer, ultrasonication, and homogenizer. The obtained products can be dried by

natural solvent evaporation, oven drying or lyophilization. The microemulsions are easily scaled up into a pharmaceutical product [2].

Nano-emulsions are thermodynamically unstable but kinetically stable, therefore, to prepare a nano-emulsion, a mechanical shearing force is necessary to separate the dispersed phase into supersmall droplets. Thus, a two-step procedure is required for the preparation of nano-emulsions. Ultrasonication, microfluidization or high-pressure homogenization following the mixing of phases will be applied to break large droplets into nano-sized ones. Besides, low energy emulsification methods including phase inversion temperature, polymorphic phase transition, self-emulsification, solvent displacement emulsification, etc. can also be applied for the synthesis of nano-emulsions [21].

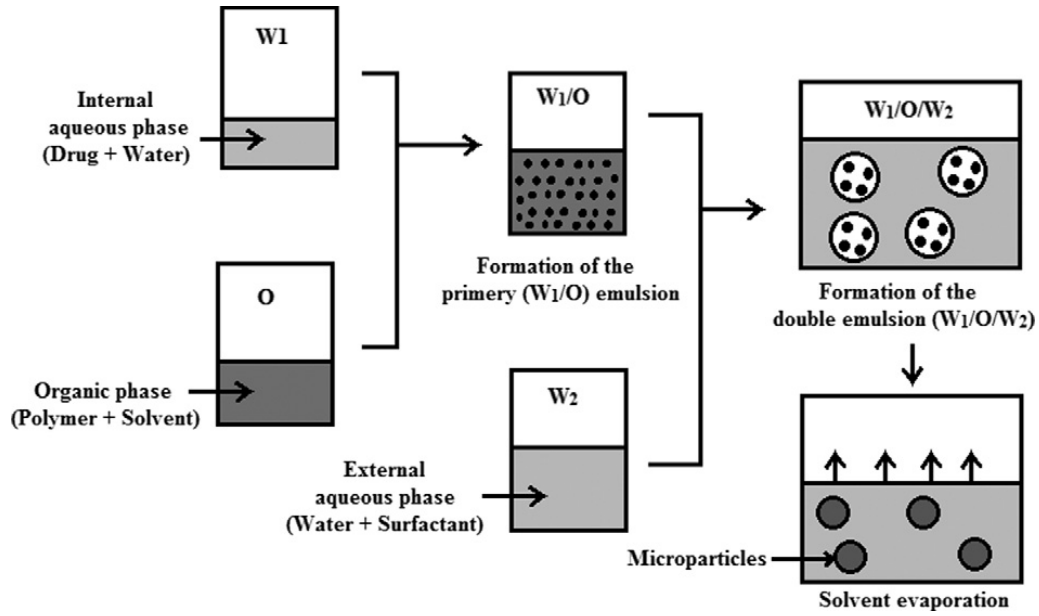

Figure 4. Procedure for preparation of solid microparticles by double emulsion solvent evaporation method. Adapted from [7].

An example of the formation of a W/O/W emulsion system which consists of an internal phase and an external phase (separated by an oil layer) is as follows. To form a stable W/O/W emulsion system, there are at least two surfactants, one has a low hydrophilic/lipophilic balance (HLB) to form a water-in-oil emulsion and the other has a higher HLB to support the second emulsion process - water in oil emulsion into water. These W/O/W emulsification systems are less viscous and are suitable candidates for controlling the release of hydrophilic drugs due to the existence of a middle oil layer that acts as a liquid membrane. The double W1/O/W2 emulsion system can be prepared in several simple steps using the double emulsion solvent evaporation method. Firstly, a hydrophilic drug is dissolved in water or suspended in water (internal aqueous phase, W1) before being emulsified in a polymer solution (O) to form the W1/O primary emulsion. Next, W1/O emulsion is dispersed in the external aqueous phase (W2) with a suitable emulsifier to form a double emulsion (W1/O/W2). Then, the mixture is solvent dried to form solid microparticles (Figure 4). The solid microparticles are separated by filtration or centrifugation before washed several times to remove the remaining emulsifiers, and vacuum dried or freeze-dried. Volatile organic solvents used for the preparation of the solid

microparticles by double emulsion solvent evaporation require a low boiling temperature to facilitate the removal of residual solvent. Common solvents for the preparation of microparticles are acetonitrile, ethyl acetate, chloroform, benzene, and methylene chloride [7].

Chitosan/polylactic acid (PLA) nanocomposites loaded with Lamivudine (an anti-HIV drug) were prepared by solvent evaporation emulsion technology based on a W/O/W emulsion system due to the hydrophilic property of Lamivudin (Figure 5) [8]. First, PLA was dissolved in dichlorometane (DCM) to form an oily phase. Next, the drug solution (W1) was dropped into the PLA solution to form a W/O emulsion. The emulsion was quickly poured into a solution of chitosan (CS) and polyethylene oxide (PEO) in 1 % acetic acid. The mixture was then ultrasonicated for 15 minutes to form a microemulsion. The microemulsion was vigorously stirred until the solvent was completely evaporated. Nanoparticles were formed by adding distilled water and icing. The product was then lyophilized to obtain dried nanoparticles. The weight of Lamivudine incorporated into the CS/PLA nanocomposite was 3 and 6 wt.%, respectively, compared with the weight of CS and PLA. The results of scanning electron microscopy (SEM) analysis showed that the morphology of CS/PLA nanoparticles and the morphology of Lamivudine-loaded CS/PLA nanoparticles were similar (Figure 6). The nanoparticles are spherical in shape with a size of 300-350 nm. The drug loading capacity of the nanoparticles reached 75.4 % and 67.9 %, corresponding to the samples containing 6 wt. % and 3 wt. % of the drug.

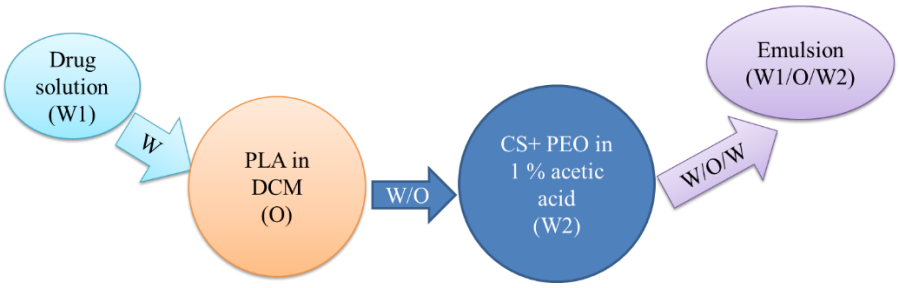

Figure 5. Procedure for synthesis of CS/PLA nanoparticles loaded with Lamivudine by solvent evaporation emulsion technology. Adapted from [8].

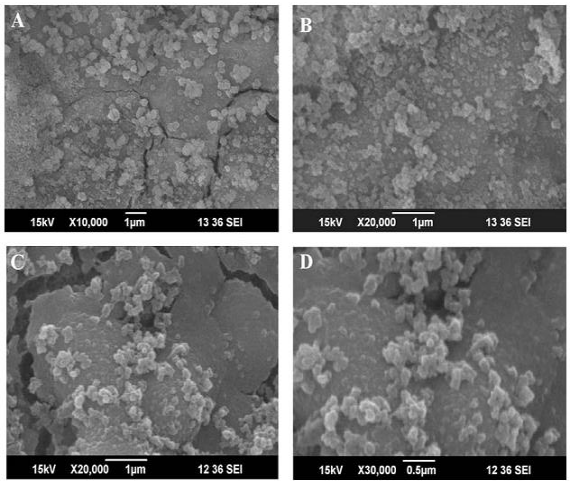

Figure 6. SEM images of CS/PLA nanoparticles (A, B) and Lamivudine-loaded CS/PLA nanoparticles (C, D). Adapted from [8].

Chitosan-polylactide composites blended with Cloisite 30 B (MMT) (80:20) which was loaded with Paclitaxel (an anti-cancer drug) were prepared by solvent evaporation emulsion technology with Paclitaxel content varying from 5, 10, 15, 20 to 25 wt.%. The composite and the drug were dissolved in chloroform. Polyvinyl alcohol (PVA) (2 % solution) was used as emulsifier. The solution of composite and drug was mixed with PVA solution and ultrasonicated for 120 seconds. The microemulsion system was kept overnight at room temperature to evaporate solvent. The solid particles were separated by centrifuging and washing with deionization water before lyophilizing [12].

Microcapsules of verapamil hydrochloride/xanthan gum (XG) were also prepared by solvent evaporation emulsion technology in an aceton/liquid paraffin solvent system [22]. Firstly, ethylcellulose, XG and drug were dispersed in acetone by ultrasonicating for 15 minutes. Next, the above mixture was poured into liquid paraffin combined with continuous stirring for 5 hours to completely remove acetone. Then, the formed microparticles were filtered and washed with n-hexane before being dried at room temperature for 24 hours. The results indicated that the average diameter of the microcapsules increased with increasing stirring rate.

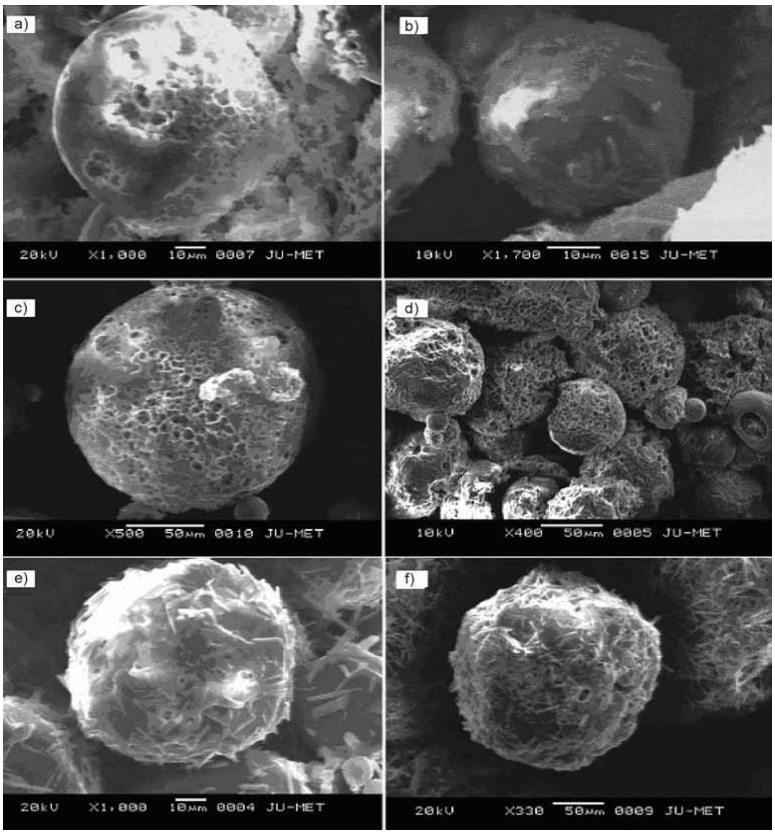

Figure 7. SEM images of porous microparticles prepared under different conditions. (a) ratio of acetone/water of 2/8 (control sample); (b) ratio of acetone/water of 0/10, ratio of drug/polymer of 0.4/1; (c) ratio of acetone/water of 2/8; (d) ratio of acetone/water of 2/8 (group microparticles); (e) ratio of acetone/water of 8/8; (f) ratio of acetone/water of 2/8, ratio of drug/polymer of 0.8/1. Adapted from [23].

XG based microsponges loading drug were also prepared by solvent evaporation emulsion method using a W/O/W emulsion system [23]. XG was gradually dispersed into an

acetone/water mixture to obtain a 0.2 % (w/v) solution. The ratio of acetone and water is about 40 - 50 % to prevent the precipitation of XG. This mixture was emulsified in a DCM solution containing 1 % (w/v) ethyl cellulose and 0.5 % (w/v) sorbitan oleate (commercial name as Span 80) on a homogenier. The W/O emulsion was then transferred to water which contained polyoxythylene esther sorbitan (commercial name as Tween 80 or polysorbate 80) on a mechanical stirrer to form a W/O/W microemulsion. The emulsion was continuously stirred to evaporate the solvent. The microsponges were separated by filtering and drying. Diclofenac sodium was used as a model drug for loading into microsponges. To form drug-loaded microsponges in a gel form, carboxypolymethylene (commercial name as Carbopol 940) was used to form thick and stable emulsions. From SEM images of the obtained samples, the polymer droplets became solid after solvent evaporation and these particles were porous (Figure 7a). However, if acetone was not used in the procedure, the microparticles were not porous (Figure 7b). The acetone/water ratio influenced the shape of microparticles, the samples prepared at an acetone/water ratio of 2/8 had the highest porosity (Figure 7 c-d). Drug crystals could be observed on the surface of microparticles when increasing the ratio of acetone/water (Figure 7e). When increasing the drug/polymer ratio, the drug crystals would exceed the surface of microparticles (Figure 7f). Since the diffusion of solvents became slower with increasing the drug/polymer ratio, the time to form drug crystals was also longer.

In our previous reports, we prepared and assessed some characteristics and the morphology of PLA/CS nanoparticles loaded with nifedipine (PLA/CS/NIF) (a calcium channel blocker medication drug) [24, 25]. PLA/CS and PLA/CS/NIF nanoparticles were prepared by microemulsion method. Firstly, oily phase and aqueous phase were prepared as follows: PLA was dissolved in DCM (oily phase - O solution); NIF was dissolved in ethanol solvent (aqueous phase - W1 solution); CS and PEO (emulsifier) were dissolved in 1 % acetic acid solution (aqueous phase - W2 solution). Next, the W1 solution was slowly dropped into the O solution and the mixture was then ultrasonicated until homogeneous. Then, the W2 solution was added to the W1/O mixture and further ultrasonicated for 60 minutes. After that, distilled water was added to the above W1/O/W2 emulsion, followed by ultrasonicating for 60 minutes and freezing for 60 minutes. Finally, the solid part was separated by centrifuging and washing with distilled water before being freeze-dried to obtain PLA/CS/NIF nanoparticles (Figure 8).

The conditions influencing the preparation of PLA/CS/NIF (PCN) nanoparticles, such as the water volume added to the W2 aqueous phase, the PEO emulsifier content, the PLA/CS ratio, and the NIF content, were investigated. The size distribution of PCN nanoparticles prepared with different water volumes added to the W2 aqueous phase in Figure 9 indicated that the size distribution of PCN nanoparticles ranged from 70 nm to 350 nm depending on the volume of distilled water used. The average particle size of PCN50 (using 50 mL of water), PCN100 (using 100 mL of water), PCN200 (using 200 mL of water), PCN250 (using 250 mL of water), PCN300 (using 300 mL of water) was 203.7 ± 7.5 nm, 163.3 ± 11.9 nm, 181.6 ± 13.3 nm, 115.8 ± 8.3 nm, and 229.4 ± 9.5 nm, respectively (Table 1). It can be seen that the most suitable volume of distilled water to be added to the W2 aqueous phase was 250 mL because the average particle size of the sample at this condition was the smallest among the tested samples. The authors also found a suitable PLA/CS ratio of 2/1 (240 mg/120 mg) and a suitable PEO content of 400 mg for the preparation of PCN nanoparticles (Table 1). At this condition, the PCN nanoparticles had a size of 115.8 ± 8.3 nm. The interactions between solvent and drug, drug and polymer, solvent and polymer under each investigation condition were different, thus, the size distributions of PCN nanoparticles were not similar [24].

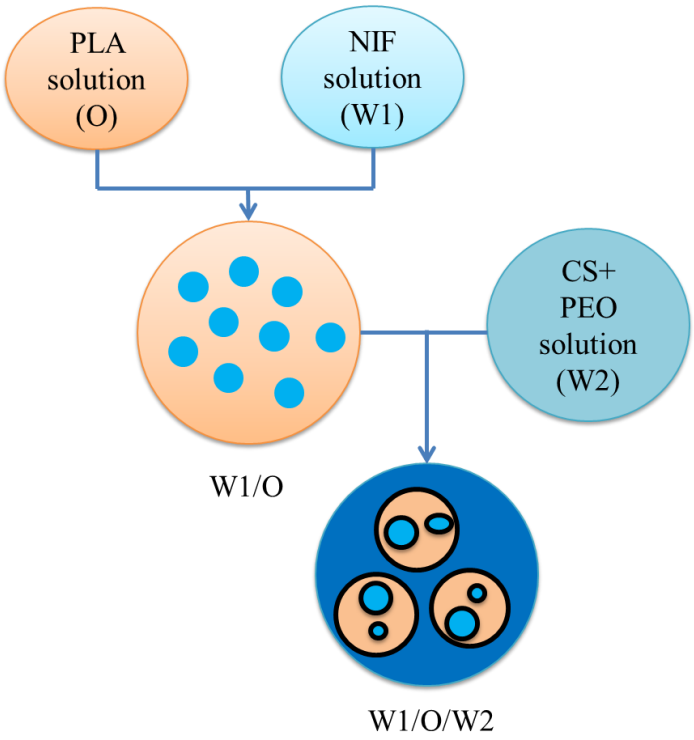

Figure 8. Procedure for preparation of PLA/CS/NIF nanoparticles.

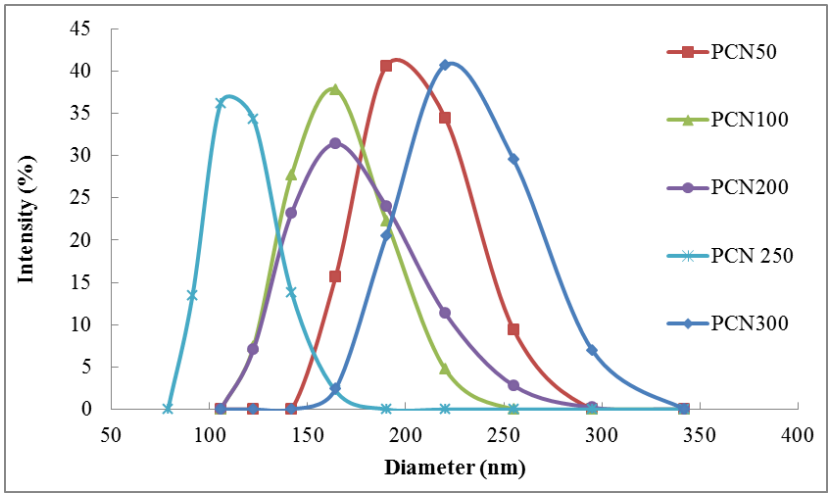

Figure 9. Size distribution of PCN prepared with different distilled water volumes added to the W2 aqueous phase. Adapted from [24].

The effect of NIF content on the characteristics of PCN nanoparticles was also investigated with the NIF content varying from 0, 10, 20, 30 to 50 wt.% compared to the PLA weight. The authors suggested that the NIF content also strongly affected the size distribution of PCN nanoparticles (Figure 10). For example, the PCN nanoparticles containing 0, 10, 20, 30 and 50 wt.% of NIF had an average particle size of 390.3 ± 64.1 nm, 187.3 ± 27.2 nm, 115.8 ± 8.3 nm, 141.0 ± 25.6 nm, and 196.1 ± 33.9 nm, respectively (Table 1). The average particle size of PCN

nanoparticles was smaller than that of PLA/CS nanoparticles without NIF loading (PC). It may be due to the formation of hydrogen bonds between NIF and polymers, leading to stronger drug-polymer interactions than drug-drug interactions [24].

Table 1. Component ratios and the average particle size of PCN nanoparticles [24].

Samples	Distilled water volume (ml)	PEO content (mg)	PLA/CS ratio	NIF content (wt.%)	Average particle size (nm)
PCN50	50	400	2/1	20	203.7 ± 7.5
PCN100	100	400	2/1	20	163.3 ± 11.9
PCN200	200	400	2/1	20	181.6 ± 13.3
PCN250 (or PCN20d)	250	400	2/1	20	115.8 ± 8.3
PCN300	300	400	2/1	20	229.4 ± 9.5
PCN200e	250	200	2/1	20	241.1 ± 18.6
PCN600e	250	600	2/1	20	241.1 ± 16.6
PCN11	250	400	1/1	20	178.0 ± 11.6
PCN12	250	400	1/2	20	405.7 ± 32.4
PC	250	400	2/1	0	390.3 ± 64.1
PCN10d	250	400	2/1	10	187.3 ± 27.2 (94.2 %) 68.0 ± 4.0 (5.8 %)
PCN30d	250	400	2/1	30	141.0 ± 25.6
PCN50d	250	400	2/1	50	196.1 ± 33.9 (95.2 %) 56.6 ± 4.5 (4.8 %)

The interaction between components in PCN20d nanoparticles was evaluated by Infrared (IR) spectroscopy and is shown in Figure 11. On the IR spectrum of PCN20d there were full peaks of the corresponding functional groups in PLA, CS and NIF. Figure 11 indicates the stretching vibration of the N-H and O-H linkages at 3332 cm^{-1}, and the stretching vibration of the C-H linkage at 2999 and 2950 cm^{-1}. The stretching vibrations of the C=O, C=C and C=C (aro) groups were assigned at 1760 cm^{-1}, 1685 cm^{-1} and 1623 cm^{-1}, respectively. In addition, the bending vibration of the N-H and NO_2 groups was recorded at 1530 cm^{-1} and 1496 cm^{-1}. The peaks at 1456 cm^{-1} and 1360 cm^{-1} were attributed to the bending vibration of the C-H linkage. The peak at 1311 cm^{-1} was assigned to the bending vibration of N-H (secondary amine). The peaks at 1189 cm^{-1} and 1092 cm^{-1} represented the secondary hydroxyl group (-CH-OH in the alcohol ring, assymmetric stretching vibration of C-O) and the primary hydroxyl group (-CH_2-OH, symmetric stretching vibration of C-O). In addition, out-of-plane vibrations of the C-H linkage were found in the wavenumber region below 1000 cm^{-1}. Comparing the peaks in the IR spectra of PLA, CS, and NIF (Table 2) [24], it can be recorgnized that the wavenumbers of the peaks characteristic of the O-H, N-H, C=O vibrations were slightly shifted, suggesting that PLA, CS and NIF in PCN20d interacted with each other through hydrogen bonding between amine and carbonyl groups in NIF with hydroxyl and carbonyl groups in polymers.

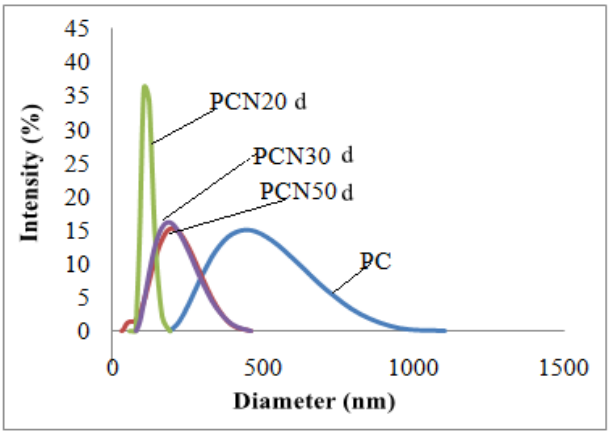

Figure 10. Size distribution of PCN prepared with different NIF contents. Adapted from [24].

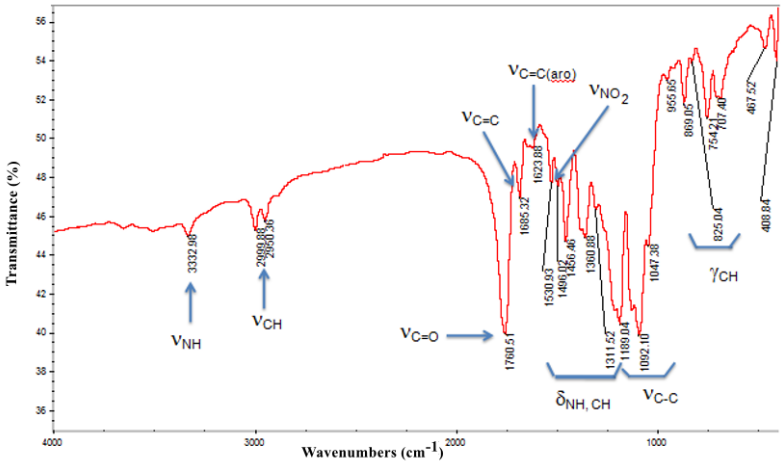

Figure 11. IR spectrum of PCN20d nanoparticles. Adapted from [24].

Table 2. Wavenumbers of some main vibrations in IR spectra of PLA, CS, NIF and PCN20d [24].

Sample / Vibration (cm^{-1})	PLA	CS	NIF	PCN20d
ν_{-NH2}, ν_{OH}	-	3365	3330	3332
ν_{CH}	2995, 2945	2950	2935	2999, 2950
$\nu_{C=O}$	1757	-	1684	1760, 1685
$\nu_{C=C\ (aro)}$	-	-	1645	1623
δ_{-NH2}	-	1559	1529	1530
δ_{-NO2}	-	-	1496	1496
δ_{CH}	1453, 1363	1412	1435, 1347	1456, 1360
ν_{C-O-C}	1185, 1092	1081	1190, 1052	1189, 1092

Figure 12 shows the SEM images of PC and PCN20d nanoparticles. It can be seen that PC and PCN20d nanoparticles have a spherical shape. The particle size of PC nanoparticles ranged from 40 to 500 nm while the size of PCN20d nanoparticles varied from 40 to 300 nm. For PCN20d nanoparticles, small particles with size from 40 to 50 nm were dominant, however they tended to agglomerate and stick together. The PCN20d nanoparticles were better separated than the PC nanoparticles. This is a reason for the reduced particle size of PCN20d nanoparticles as compared to PC nanoparticles [24 - 25].

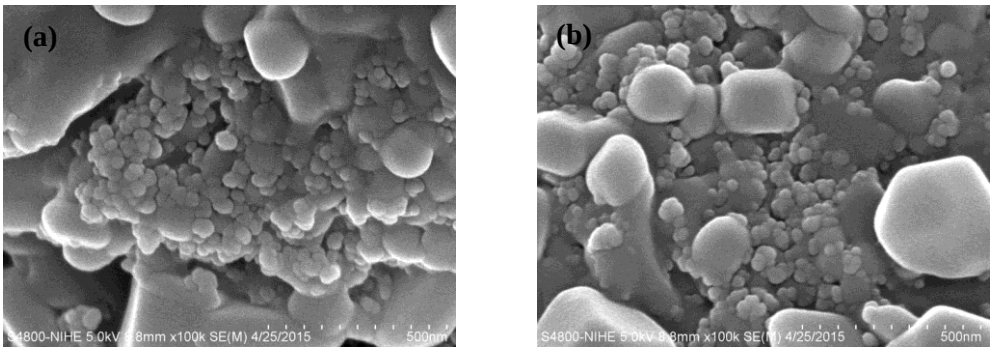

Figure 12. SEM images of PC (a) and PCN20d (b) nanoparticles. Adapted from [24].

Transmission electron microscopy (TEM) images of PC and PCN20d nanoparticles are presented in Figure 13. The PC and PCN20d nanoparticles are spherical, solid, and homogeneous.

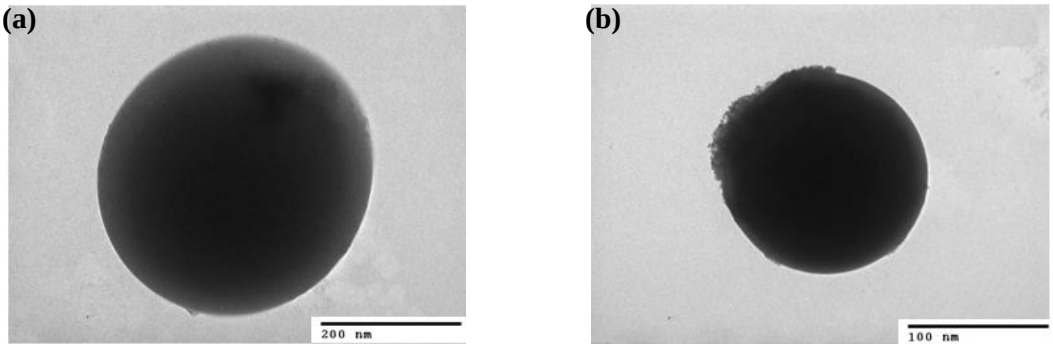

Figure 13. TEM images of PC (a) and PCN20d (b) nanoparticles. Adapted from [24].

The X-ray diffraction (XRD) pattern of NIF, PC and PCN nanoparticles revealed crystal peaks with a strong intensity of NIF at 2θ of 16, 19.56 and 24.55 Å. The two broad crystal peaks at 2θ of 16.59 Å and 19.01 Å corresponded to the (200) and (110) rhombic crystal planes of PLA and CS in the PC nanoparticle, respectively. The crystal peaks of PLA and CS on the XRD pattern of PCN nanoparticles were slightly shifted with much higher intensity than the corresponding peaks on the XRD pattern of PC nanoparticles. For instance, the crystal peak of PLA was located at 2θ of 16.62, 16.71, 16.57, and 16.53 Å for PCN10d, PCN20d, PCN30d, and PCN50d nanoparticles, respectively. This result showed that PCN nanoparticles had greater crystallinity than PC nanoparticles due to the good interaction between PLA, CS and NIF as

aforementioned. When increasing the NIF content in PCN nanoparticles, the crystal peaks of PLA and CS became more broaden, corresponding to an increase in the relative crystallinity of these samples. Besides, the intensity of the NIF crystal peaks also increased with increasing the NIF content in the nanoparticles [24]. PCN nanoparticles containing different NIF contents were hydrophilic with contact angle less than 90^o [26]. The nanoparticles had a rough surface and did not contain heavy metal ions. The swelling ability in phosphate buffer of PCN nanoparticles was better than that of PC nanoparticles [26]. The drug loading capacity of PCN nanoparticles was also determined. The drug loading capacity of PCN10d, PCN20d, PCN30d, and PCN50d nanoparticles was 98.7, 98.3, 99.0, and 88.6 %, respectively [24]. These values were quite high, suggesting that the W/O/W emulsion method is suitable for the preparation of NIF-loaded PLA/CS nanoparticles.

In another paper, we synthesized PLA/CS/NIF nanoparticles with CS nanoparticles containing NIF as the core and PLA as the shell [27]. The CS nanoparticles loaded with NIF were prepared by emulsion method from a microemulsion containing NIF, CS, PEO, 1 % acetic acid, ethanol, and DCM. The particle size of CS/NIF nanoparticles was 230.2 nm and 164.2 nm corresponding to the NIF content of 30 and 50 wt.%, respectively. The Zeta potential of CS/NIF nanoparticles was positive, in which CS/30 wt.% NIF nanoparticles were more stable in water than CS/50 % NIF nanoparticles.

D. Jeevitha and K. Amarnath synthesized CS/PLA nanoparticles loaded with anthraquinone by emulsion method [28]. The CS/PLA nanoparticles had a heterogenous structure with irregular shape and size and had microholes while anthraquinone-loaded CS/PLA nanoparticles had a regular structure with the particle size lower than 200 nm. The drug-loaded nanoparticles had a core-shell structure, in which CS was the core and PLA-anthraquinone was the shell.

Nguyen Thi Thu Trang, Thai Hoang *et al.* prepared PLA/CS nanoparticles loaded with quinine and hydroquinine by emulsion method in the presence of polycaprolactone (PCL) or polyethylene oxide (PEO) as an emulsifier [29, 30]. The oily phase was prepared by dissolving PLA and PCL in DCM. The first aqueous phase was formed by dissolving drug in ethanol. The W1 solution was poured into the O solution to form a W1/O emulsion. Next, the W1/O emulsion was poured into the second aqueous phase containing CS dissolved in 1 % acetic acid. The mixture was then stirred for 15 minutes in a microwave-assisted system reactor (MAS-II) (Figure 14) to form a microemulsion. The emulsion was vigorously stirred until the organic solvent was completely evaporated. The nanoparticles were formed after adding distilled water to the emultion and freezing. After that, the solid part was separated by centrifugating and washing with distilled water before lyophilizing. The IR results indicated that quinin interacted with PLA and CS through physical interaction such as hydrogen bonding or dipole-dipole interaction between functional groups of quinin and that of PLA and CS. The PLA/CS/quinin and PLA/CS/hydroquinine nanoparticles were spherical in shape [29, 30]. The PLA/CS/quinin nanoparticles had a size of 60 nm to 200 nm, depending on the quinin content. The drug loading capacity of PLA/CS/quinin nanoparticles reached 38.9 to 82.2 %. The PLA/CS nanoparticles containing 10 wt.% of quinin had the highest drug loading capacity [24]. The particle size of PLA/CS nanoparticles loaded with hydroquinine was larger than that of PLA/CS nanoparticles loaded with quinine. The size of hydroquinine-loaded PLA/CS nanoparticles ranged from 70 nm to 200 nm. The hydroquinine loading capacity of PLA/CS nanoparticles was higher than the quinin loading capacity [30].

Figure 14. Microwave-assisted system reactor (MAS-II).

The rifampicine-loaded CS/PLA nanoparticles prepared by emulsion method had a spherical shape, regular density and high porousity. The nanoparticles had a size of 187 nm and a Zeta potential of 21 ± 2.2 mV. The particle size of the nanoparticles was also dependent on the content of rifampicine as well as the interaction between rifampicine and the surface of CS-PLA. When adding polyethyleneglycol (PEG) to the CS/PLA/rifampicine emulsion system, the size and Zeta potential of the nanoparticles changed negligibly. The authors suggested that the saturated content of rifampicine in the CS/PLA nanoparticles was 50 wt.% because when increasing the drug content beyond 50 wt.%, the stability and Zeta potential of the nanoparticles remained unchanged while the particle size increased sharply [31].

Thapa Chhitij *et al.* have optimized the conditions for the preparation of SMEDDS containing coenzyme Q_{10} [32]. By D-optimal mixture design, the authors found the optimal formulation for SMEDDS based on the solubility and concentration of these systems. The formulation under optimal conditions consists of omega-3 (oil phase, 38.55 %), Lauroglycol®90 (co-surfactant, 31.42 %), and Gelucire 44/14 (surfactant, 30 %). The mean size of droplets was 237.6±5.8 nm and the solubilization of coenzyme Q_{10} was 16±2.48 %. The solubility of coenzyme Q_{10} in phosphate buffer medium (pH 6.8) was significantly enhanced when loaded into SMEDDS.

Ashok Kumar Janakiraman *et al.* reported that the SMEDDS containing capryol 90, PEG 400, and labrasol could remarkably improve the stability and solubility of Vorinostat drug [33]. Vorinostat was dissolved in capryol 90 and mixed with a vortex mixer for 20 minutes to form an oily phase. PEG 400 and labrasol were then introduced into the above mixture and mixed for 20 minutes. Next, the mixture was kept at 30 ± 0.5 ^{o}C in a water bath for 30 minutes. The solid part was sonicated and stored at room temperature. The mean droplet size and Zeta potential of this system were 272.9 ± 82.7 nm and -57.2 mV, respectively.

Tran Do Mai Trang, Thai Hoang *et al.* prepared chitosan/collagen nanocomposites loaded with lovastatin (a treatment drug for lowering total cholesterol in the blood) by emulsification

method [34]. The aqueous phase was formed by mixing a solution of collagen, CS, PEO in 1 % acetic acid with a solution of lovastatin in ethanol. The oily phase is DCM solution. Distilled water was added to the emulsion mixture to remove residual PEO. The emulsion was iced for 120 minutes to form nanoparticles. The nanoparticles were then separated by centrifugating and washing with distilled water before lyophilization. The designation and weight of components in chitosan/collagen nanocomposites containing lovastatin (abbreviated as CCL) is presented in Table 3. CCL nanoparticles had an average particle size of 137.0 - 444.0 nm and a drug loading capacity of 89.6 to 99.5 % depending on the composition ratio in the samples. CCL2 nanoparticles had the smallest average particle size (137 nm) and high drug loading capacity (98.7 %). CCL5 nanoparticles had the highest drug loading capacity (99.5 %).

Table 3. Designation and weight of components in chitosan/collagen nanocomposites loaded with lovastatin [34].

No.	Designation	Chitosan weight		Collagen weight		Lovastatin weight	
		g	%	g	%	g	%
1	CCL1	0.100	69.366	0.024	16.761	0.020	13.873
2	CCL2	0.100	60.910	0.024	14.720	0.040	24.370
3	CCL3	0.100	78.690	0.012	9.510	0.015	11.800
4	CCL4	0.100	70.387	0.012	8.501	0.030	21.112
5	CCL5	0.100	45.450	0.100	45.450	0.020	9.100
6	CL	0.100	90.909	0.000	0.000	0.010	9.091

5. RELEASE OF DRUG FROM THE PARTICLES PREPARED BY EMULSION TECHNIQUES

The mechanism for drug release from the particles obtained from emulsions is quite complex, depending on the concentration of particles in the medium, the dose of drug, pH of medium, nature of drug and polymers, size of particles, properties of particles, and so on. The popular kinetic models for studying drug release process from the particles in the medium include zero order kinetics, first order kinetics, Higuchi, Hixson Crowel, Korsmeyer-Peppas, Heller-Baker, Ritger-Peppas, etc. Liu *et al.* tested the release of ginsenoside Rg3 from PLA/ginsenoside Rg3 microspheres in a phosphate buffer medium (pH 7.4) at 37 ^{o}C [11]. They found that it was easy to release ginsenoside Rg3 from the microspheres, the drug release rate reached 68 % and 89 % after 2 hours and 6 hours of testing, respectively. After 6 hours of testing, the drug release became slow. The drug release was found to follow two stages: fast-release stage involving the release of drug from the surface of microspheres and slow-release stage associated with the diffusion of drug inside the microspheres to the medium. The authors calculated the correlation coefficient from regression equations related to the release of ginsenoside Rg3 from microspheres (Table 4). The Heller-Baker model gave the best fit for the release of ginsenoside Rg3 from microspheres in the phosphate buffer medium (pH 7.4) at 37 ^{o}C.

Table 4. Regression equation and correlation coefficient of models reflecting the release of ginsenoside Rg3 from PLA/ginsenoside Rg3 microspheres [11].

No	Model	Regression equation	Correlation coefficient
1	First order	$w = 0.364 + 0.113t$ (3)	0.790
2	Heller-Baker	$w = 0.921 – \exp(-0.685t)$(4)	0.979
3	Higuchi	$w = 0.069 + 0.0383t^{1/2}$ (5)	0.910
4	Hixson-Crowell	$(35.622 + w)^{1/3} = 3.302 + 0.003t$ (6)	0.788
5	Ritger-Peppas	$w = -273.958 + 274.411t^{0.001}$ (7)	0.974

Table 5. Parameter kinetics of Paclitaxel release process from the nanoparticals in pH 1.2 and pH 7.4 media [12].

Drug content, %	*K*	*n*	Correlation coefficient, R^2
pH 7.4			
5	0.08	0.50	0.964
10	0.04	0.55	0.968
15	0.07	1.68	0.961
20	0.25	1.55	0.955
25	0.29	1.66	0.963
pH 1.2			
5	0.24	0.48	0.979
10	0.02	0.54	0.944
15	0.19	1.55	0.978
20	0.04	1.67	0.969
25	0.20	1.88	0.991

Nanda *et al*. reported that the drug release from the PLA/CS/MMT nanoparticles depended on pH of the medium [12]. When increasing pH of the medium from 1.2 to 7.4, the concentration of Paclitaxel released from the nanoparticles to the medium increased. For example, after 15 hours of testing in pH 1.2 medium, the amount of Paclitaxel released reached 30.8, 36.95, 38.18, 38.37, and 48.52 % corresponding to samples containing 5, 10, 15, 20, and 25 wt.% of the drug. Meanwhile, the content of Paclitaxel released from these samples was 40.15, 44.71, 47.89, 56.09, and 64.63 %, respectively. The drug release mechanism of Paclitacel from the nanoparticles complied with Korsmeyer-Peppas model with rate constant (K) and diffusion coefficient (n) values presented in Table 5. The value of n ranged from 0.55 to 1.68 suggesting that the transformation of Paclitaxel from the nanoparticles took place from a non-Fickian form to an irregular form.

Dev *et al*. also studied the release of Lamivudine from PLA/CS nanoparticles in pH 1.2, pH 7.4, and pH 10.5 media [8]. Two tested samples showed the same trend in drug release process. After 12 hours of testing, the PLA/CS nanoparticles containing 3 wt.% of Lamivudine released 50.1, 60.5, and 64.6 %, corresponding to pH 1.2, pH 7.4, and pH 10.5 media, respectively. The nanoparticles loaded with 6 wt.% of the drug, the drug release content reached 59.5 % to 66.1 % after 12 hours of testing in these above media.

The release of NIF from PLA/CS nanoparticles depended on pH of the medium, content of NIF, and testing time. The release mechanism of NIF from PLA/CS nanoparticles was complex and followed the power law equation (highest regression coefficients) with the Fick diffusion mechanism (Tables 6 and 7) [24].

Table 6. Regression coefficients (R^2) of kinetic equations of PCN nanoparticles in pH 7.4 medium [24].

Samples	Zero - order	First - order	Hixson-Crowell	Higuchi	Power law	
	R^2	R^2	R^2	R^2	n	R^2
PCN10d	0.9467	0.7181	0.9182	0.9906	0.279	0.9988
PCN20d	0.9786	0.8558	0.9172	0.9958	0.342	0.9948
PCN30d	0.9334	0.8338	0.9097	0.9747	0.261	0.9958
PCN50d	0.9183	0.6316	0.8219	0.9769	0.276	0.9918

Table 7. Drug release rate constant, diffusional constant and regression coefficients (R^2) of power law equation of PCN nanoparticles in different pH solutions [24].

Samples	pH 6.8			pH 2.0			pH 1.2		
	k	n	R^2	k	n	R^2	k	n	R^2
PCN10d	0.781	0.274	0.9960	0.764	0.322	0.9509	0.778	0.293	0.9392
PCN20d	0.801	0.242	0.9938	0.800	0.244	0.9913	0.791	0.258	0.9790
PCN30d	0.716	0.375	0.9807	0.761	0.313	0.9516	0.733	0.339	0.9794
PCN50d	0.718	0.376	0.9669	0.688	0.405	0.9879	0.741	0.331	0.9309

Table 8. Content of lovastatin released from chitosan/collagen/lovastatin (CCL5) nanoparticles and chitosan/lovastatin (CL) nanoparticles in different pH media [34]

Time (hour)	pH = 7.4		pH = 6.8		pH = 4.5		pH =2.0	
	CCL5	CL	CCL5	CL	CCL5	CL	CCL5	CL
1	46.98	21.49	38.37	18.49	30.42	10.30	28.00	9.64
2	50.87	28.20	41.05	21.36	32.83	17.17	29.32	11.84
3	52.17	31.56	42.84	27.09	35.23	18.32	31.29	14.66
4	57.36	34.92	44.63	28.52	40.03	24.04	33.92	16.54
5	62.55	38.27	49.99	32.82	45.64	27.48	35.89	17.48
6	67.74	40.51	54.47	37.12	48.84	29.77	37.20	23.12
7	74.23	44.99	57.15	39.99	53.64	36.64	39.18	26.88
8	78.12	48.35	65.20	42.86	61.65	37.78	41.80	28.76
9	80.72	50.58	66.99	45.73	64.05	42.36	46.41	34.40
10	84.61	62.89	69.67	50.03	67.26	48.09	60.21	40.04
11	87.21	69.61	75.93	58.63	73.66	53.81	66.13	50.38
12	88.51	71.85	79.51	61.49	76.86	56.10	68.76	53.20
24	91.10	72.97	83.98	65.79	79.27	58.39	70.73	56.96
28	92.40	75.21	85.77	68.66	80.87	61.83	72.70	60.72
32	94.99	76.33	86.67	71.53	81.67	64.12	74.67	62.60

The content of lovastatin released from chitosan/collagen/lovastatin (CCL5) nanoparticles and chitosan/lovastatin (CL) nanoparticles in different pH media is presented in Table 8 [34]. The release of lovastatin depended on the pH of the medium, composition of the nanoparticles and time of testing. The drug release of lovastatin from CCL5 and CL nanoparticles followed two stages including a fast-release stage and a controlled release stage. In the pH 7.4 medium, the drug released from the nanopartilces complied with the zero order kinetic model while in pH 2 and pH 6.8 media, the release of drug followed the frist order kinetic equation. In the pH 4.5 medium, the Hixson-Crowell was suitable to drug release from the nanoparticles. The mechanism of drug release from CCL nanoparticles followed the diffusion mechanism of Fick's law.

SNEDDS of sunitibib malate were prepared, characterized and evaluated for the *in-vitro* dissolution rate and anticancer efficacy [35]. The authors found the optimal conditions for the preparation of SNEDDS of sunitibib malate. After 24 hours of testing in a phosphate buffer medium, the drug release content from SNEDDS reached 95.4 %, much higher than that from SNEDDS unloaded with sunitibib malate.

6. *IN-VIVO* TEST OF PARTICLES OBTAINED BY MICROEMULSION TECHNIQUES

There are different routes of administration for the emulsion drug delivery such as oral delivery, intravenous delivery, topical delivery, ocular delivery, or nasal delivery as shown in Figure 15 [21].

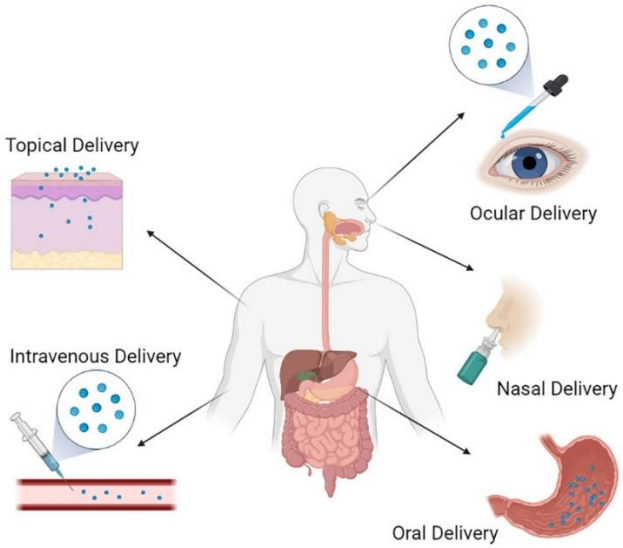

Figure 15. Strategies of administration of emulsion drug delivery. Adapted from [21].

When applying oral administration on rats, PLA/CS/NIF nanoparticles exhibited a positive efficacy in lowering blood pressure in rats, demonstrating a faster and longer lasting effect in terms of arterial pressure than NIF-unloaded nanoparticles [26]. The PLA/CS/NIF nanoparticles caused a slight decrease in heart rate in the late stages, without affecting the depolarization of mouse cardiomyocytes. They had no side effects on the hematopoietic functions, respiratory system, and nervous system of rats. The PLA/CS/NIF nanoparticles were safe with LD_{50} on rats of 700 mg/kg. When using the nanoparticles with a dose of 3 mg/kg/day and 15 mg/kg/day, they did not cause semi-toxicity on rats.

Vorinostat-loaded SMEDDS formulation exhibited the significant performance in solubility and bioavailability as compared to Vorinostat-unloaded SMEDDS. The SMEDDS gave a higher absorption rate in GI thanks to opening the tight junctions in the intestine, leading to an increase in intestinal wall permeability [33].

CCL5 nanoparticles did not cause acute toxicity in rats when used at doses higher than 1000 mg/kg. The hematopoietic function as well as liver and kidney functions of rats after 28 days of testing with CCL5 nanoparticles were not affected. These nanoparticles are potential for application in drug delivery [34].

Rhamnolipid-coated W/O/W double emulsion nanoparticles loaded with doxorubicin/erlotinib were successfully systhesized by Lee *et al.* [36]. The nanoparticles contained both doxorubicine (hydrophilic drug) and erlotinib (hydrophobic drug) and were found to exhibit a synergetic effect on the treatment of tumor tissue and tumor therapy, suggesting that the double emulsion method was potential for combination of hydrophobic and hydrophilic drugs in the nanoparticles, in which rhamnolipid was used as a biosurfactant for the emulsion system. The nanoparticles exhibited a high accumulation in SCC7 tumor tissue in rats after intravenous injection (Figure 16).

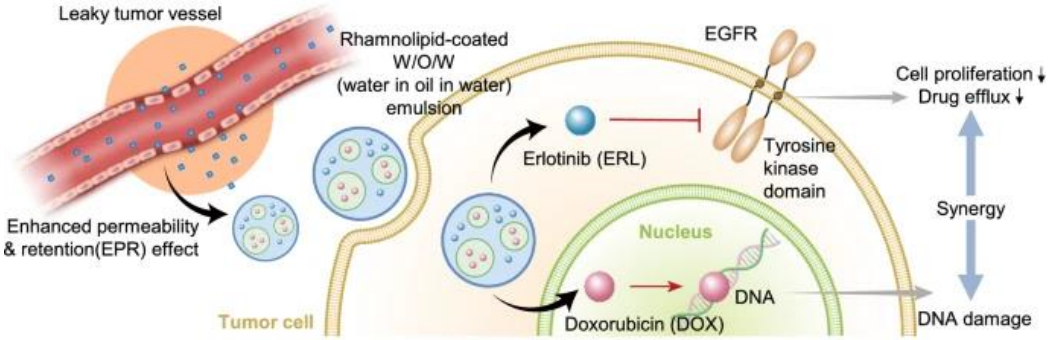

Figure 16. Effect of rhamnolipid-coated W/O/W double emulsion nanoparticles loaded with doxorubicin/erlotinib in cancer treatment. Adapted from [36].

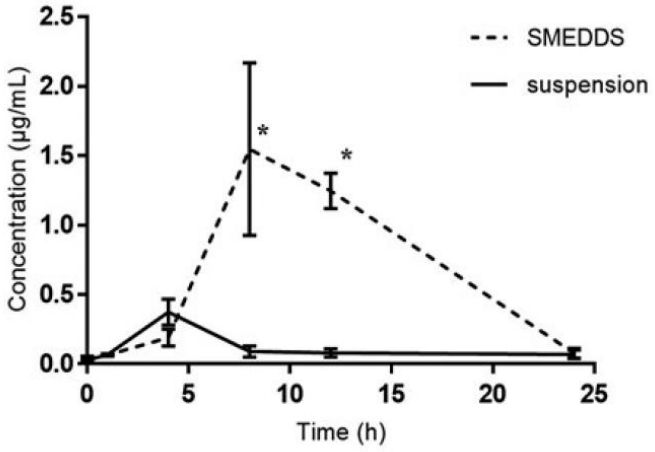

Figure 17. Concentration of coenzyme Q_{10} with oral administration with coenzyme Q_{10} SMEDDS and coenzyme Q_{10} suspension formulations in rats. Adapted from [32].

The bioavailability of coenzyme Q_{10} loaded by the SMEDDS was also improved as compared to coenzyme Q_{10} unloaded by the SMEDDS [32]. The concentration of coenzyme Q_{10} in blood when administrated with coenzyme Q_{10} SMEDDS was much higher than that when administrated with coenzyme Q_{10} suspension (Figure 17). The area under the curve of coenzyme Q_{10} was 17.42 ± 2.3 (µg.h/mL) and 3.8 ± 1.3 (µg.h/mL) after oral administatrion for 24 hours with an equivalent dose of 60 mg/kg of coenzyme Q_{10} SMEDDS and coenzyme Q_{10} suspension, respectively. The maximum concentration of coenzyme Q_{10} when treated with coenzyme Q_{10} SMEDDS reached 1.54 ± 0.62 (µg/mL) after 8 hours of oral administration while the maximum concentration of coenzyme Q_{10} when treated with coenzyme Q_{10} suspension reached only 0.37±0.09 (µg/mL) after 4 hours of treatment. The authors found the relative bioavailability of coenzyme Q_{10} SMEDDS was 458.42 %.

The emulsion systems are also potential for application in skin drug delivery because they help to improve the permeation of drugs through the skin [37 - 39]. The O/W emulsion containing chitosan, tween 80, span 80, octylmethoxycinnamate, octocrylene, diethylamino hydroxybenzoyl hexyl benzoate, benzophenone-3, and pomegranate extract was used to increase skin retention and photoprotection [38]. The experimental model has been applied on rats.

Gupta *et al.* studied the effectiveness of paclitaxel loaded perfluorocarbon/poly(ethylene oxide)-co-poly(d,l-lactide) (PEG-PDLA) nanoemulsions in the treatment of tumor. The paclitaxel loaded nanoemulsions did not cause hematological toxicity on rats and had a strong therapeutic effect with complete tumor resolution of rats after the rats were injected 15 times with the same dose of 1% PFCE/2 % PEG-PDLA/0.5 % PTX nanoemulsion formulation (twice a week for 7.5 weeks) [40].

Haggag *et al.* showed that the insulin-loaded nanoparticles prepared from 10 % of PEG-PLGA (poly(D,L-lactic-co-glycolic acid) emulsion maintained normoglycaemia for 24 hours in diabetic rats following a single bolus, with no evidence of hypoglycemia [41].

Chaudhary *et al.* prepared SNEDDS loaded with nabumetone by emulsification method using capryol 90, tween 80 and PEG 400. *In-vivo* tests on rats showed the improved oral bioavailability and better anti-inflammatory effect of nabumetone from SNEDDS [42].

Echeverri *et al.* synthesized nanoemulsions loaded with carbamazepine drug via ultra-high-pressure homogenization [43]. Experiments on rats indicated that the nanoemulsions significantly improved the drug absorption time in blood, from 12 hours for coarse emulsion to 45 minutes for nanoemulsion formulations.

The nanoemulsions were made by mixing the internal oily phase containing artemether drug dissolved in coconut oil and span 80 with the external aqueous phase containing tween 80, ethanol and water. The obtained nanoemulsions had a spherical shape, an average size of 79 nm, and high stability. The oral bioavailability of the nanoemulsion formulation was 2.6 times higher than the plain drug [44].

Rapoport *et al*. indicated that the PFCE nanoemulsions greatly improved the efficacy of paclitaxel in the treatment of breast and pancreatic cancer in rats [45].

7. RESEARCH DIRECTIONS IN COMING TIME

The emulsification method has been widely applied in the preparation of polymeric drug delivery. The nanoparticles or microspheres obtained from the emulsion formulations could greatly control drug release process, enhance the solubility, bioavailability, and treatment efficacy of the drugs. In particular, the most part of new drugs has the nature of low aqueous

solubility, unstable and poor bioavailability. Therefore, the development of new emulsion formulations for loading hydrophilic drugs, hydrophobic drugs or both hydrophilic and hydrophobic drugs is still very novel in the scientific world. In addition, the optimization of emulsion processing by software facilitates experiments. Moreover, clinical trials of emulsion formulations in animals and humans need to be approved to open up practical applications of these formulations.

8. CONCLUSION

Emulsification is certainly a promising strategy for drug administration and delivery. Microemulsions, nanoemulsions or self-emulsifying drug delivery systems (SEDDS) are effective carriers to improve the solubility, release rate, bioactivity, and bioavailability of drugs in research and treatment. The emulsification method is quite simple and can be scaled up to industry. The ingredients of emulsion systems as well as drugs can be varied to choose from. The comparison of the efficacy of microemulsions, nanoemulsions, and SEDDS is necessary for research to distinguish them unequivocally, which is the best method for theraputic application.

CRediT authorship contribution statement. Nguyen Thuy Chinh: Methodology, Writing manuscript, Conceptualization, Formal analysis. Thai Hoang: Supervision, Conceptualization, Review and editing, Formal analysis.

Declaration of competing interest. The authors declare that they have no known competing financial interests or personal relationships that could have appeared to influence the work reported in this paper.

ABREVIATION

CCL: Chitosan/collagen nanocomposites loaded with lovastatin
CL: Chitosan/lovastatin
CS: Chitosan
DCM: Dichloromethane
GI: Gastrointestinal
HLB: Hydrophilic/lipophilic balance
IR: Infrared
MMT: Montmorillonite
NIF: Nifedipine
O: Oil
PC: PLA/CS nanoparticles unloading NIF
PCL: polycaprolactone
PCN: Polylactic acid/chitosan/nifedipine
PEG: Polyethyleneglycol
PEG-PDLA: Poly(ethylene oxide)-co-poly(d,l-lactide)
PEO: Polyethylene oxide
PFCE: Perfluorocarbon
PLA: Polylactic acid
PLGA: Poly(D,L-lactic-co-glycolic acid)
PVA: Polyvinyl alcohol
SEDDS: Self-emulsifying drug delivery system
SEM: Scanning electron microscopy
SES: Self-emulsifying systems

SMEDDS: Self-microemulsifying drug delivery system
SNEDDS: Self-nanoemulsifying drug delivery system
TEM: Transmission electron microscopy
W: Water
XG: Xanthan gum

REFERENCES

1. Guti´ errez J. M., Gonz´ alez C., Maestro A., Sol` e I., Pey C. M., Nolla J. - Nano-emulsions: New applications and optimization of their preparation, Curr. Opin. Colloid. Interface Sci. **13** (2008) 245-251.
2. Wang X. Q. and Zhang Q. - Microemulsions for drug solubilization and delivery, in: Dennis D. and Alfred F. (Eds.), Drug Delivery Strategies for Poorly Water-Soluble Drugs, John Wiley & Sons, Ltd, 2013.
3. Hoar T. P., Schulman J. H. - Transparent water-in-oil dispersions: the oleopathic hydro-micelle, Nature. **152** (1943) 102-103.
4. Schulman J. H., Stoeckenius W., Prince L. M. - Mechanism of formation and structure of microemulsions by electron microscopy, J. Phys. Chem. **63** (1959) 1677-1680.
5. Solans C., Izquierdo P., Nolla J., Azemar N., Garcia-Celma M. J. - Nano-emulsions, Curr. Opin. Colloid. Interface Sci. **10** (2005) 102–110.
6. Jones M. C., Leroux J. C. - Polymeric micelles: A new generation of colloidal drug carriers, Eur. J. Pharm. Biopharm. **48** (1999) 101-111.
7. Tapan K. G., Chhatrapal C., Ajazuddin A. A., Hemant B., Dulal K. T. - Review: Prospects of pharmaceuticals and biopharmaceuticals loaded microparticles prepared by double emulsion technique for controlled delivery, Saudi Pharm. J. **21** (2013) 125-144.
8. Dev A., Binulal N. S., Anitha A., Nair S. V., Fruike T., Tamura H., Jayakumar R. - Preparation of poly(lactic acid)/chitosan nanopaticles for anti - HIV drug delivery applications, Carbohydr. Polym. **80** (2010) 833-838.
9. Sahoo S., Sasmal A., Nanda R., Phani A. R., Nayak P. L. - Synthesis of chitosan–polycaprolactone blend for control delivery of ofloxacin drug, Carbohydr. Polym. **79** (2010) 106-113.
10. Han S., Li M., Liu X., Gao H., Wu Y. - Construction of amphiphilic copolymer nanoparticles based on gelatin as drug carriers for doxorubicin delivery, Colloids Surf. B: Biointerface **102** (2013) 833-841.
11. Liu C., Zhang D., Li D., Jiang D., Chen X. - Preparation and characterization of biodegradable polylactide(PLA) microspheres encapsulating ginsenoside Rg3, Chem. Res. Chinese Universities **24** (5) (2008) 588-591.
12. Nanda R., Sasmal A., Nayak P. L. - Preparation and characterization of chitosan - polylactide composites blended with Cloisite 30B for control release of the anticancer drug Paclitaxel, Carbohydr. Polym. **83** (2011) 988-994.
13. Khanna S., Katare O. P., Nasa A., Garg A. - Microemulsions: Developmental aspects, Res. J. Pharm. Biol. Chem. Sci. **1** (2010) 683-706.
14. Robbins M. L. - Theory of microemulsion, AIChE Symp. Ser. **40**A (1974) 1-17.

15. Thomas Z. - Flexibility, persistence length and bicontinuous microstructures in microemulsions, C. R. Chim. **12** (1-2) (2009) 218-224. https://doi.org/10.1016/j.crci.2008.10.008
16. Constantinides P. P. - Lipid microemulsions for improving drug dissolution and oral absorption: Physical and biopharmaceutical aspects, Pharm. Res. **12** (1995) 1561-1572.
17. Gibaud S., and Attivi D. - Microemulsions for oral administration and their therapeutic applications, Expert Opin. Drug Deliv. **9** (2012) 937-951. doi:10.1517/17425247.2012.694865.
18. Mori D., Poonam V., Kajal P., Keshvi S., Mohini P., Sushma P., Kiran D., Sunny S., Ravi M., Ramesh P. - Lipid-based emulsion drug delivery systems - a comprehensive review, Drug Deliv. Transl. Res. **12** (2022) 1616-1639. https://doi.org/10.1007/s13346-021-01071-9
19. Nida S., Alzahrani A. K., Jamith Basha W., Nadeem K., Arsalan Z., Jaweria A., and Hassan M. K. - Microemulsions: Unique properties, pharmacological applications, and targeted drug delivery, Front. Nanotechnol, Sec. Biomedical Nanotechnol., 2021, https://doi.org/10.3389/fnano.2021.754889.
20. Cynthia A. C. - Lipids for self-emulsifying drug delivery systems, Pharm. Technol. **45** (11) (2021) 20-24.
21. Russell J. W., Yang L., Guangze Y., Chun-Xia Z. - Nanoemulsions for drug delivery, Particuology **64** (2022) 85-97, https://doi.org/10.1016/j.partic.2021.05.009.
22. Wanjari B. E., Gaikwad N. J. - Development and evaluation of verapamil hydrochloride xanthan gum microcapsules as controlled drug delivery system, Int. J. Pharm. Sci. Res. **3** (9) (2012) 3296-3303.
23. Sabyasachi M., Santanu K., Somasree R., Biswanath S. - Development and evaluation of xanthan gum-facilitated ethyl cellulose microsponges for controlled percutaneous delivery of diclofenac sodium, Acta Pharm. **61** (2011) 257-270.
24. Chinh N. T., Trang N. T. T., Giang N. V., Thanh D. T. M., Hang T. T. X., Tung N. Q., Truyen C. Q., Quan P. M., Long P. Q., and Hoang T. -*In vitro* nifedipine release from poly(lactic acid)/chitosan nanoparticles loaded with nifedipine, J. Appl. Polym. Sci. **133** (16) (2016) 43330. https://doi.org/10.1002/app.43330.
25. Trang N. T. T., Chinh N. T., Mai T. T., Hoang T. - Study on characteristics, properties and morphology of polylactic acid/chitosan nanoparticles prepared by emulsification method, Vietnam J. Chem. **54** (3) (2016) 269 -273. (in Vietnamese)
26. Chinh N. T., Trang N. T. T., Mai T. T., Thanh D. T. M., Trung T. H., Trung T. H., Quan L. V., Hoa N. T., Mao C. V., Nghia N. T., *et al.* - Polylactic acid/chitosan nanoparticles carrying nifedipine: Some physical characteristics and in vivo test results in animal, J. Nanosci. Nanotechnol. **18** (2018) 2294-2303.
27. Chinh N. T., Duc L. N., Trung T. H., Huynh M. D., Giang N. V., Cong D. V., Mai T. T., Lam T. D., and Hoang T. - Synthesis and characterization of core–shell structure PLA/CS/NIF nanoparticles, Int. J. Nanotechnol. **15** (Nos 11/12) (2018) 952-967.
28. Jeevitha D., Amarnath K. - Chitosan/PLA nanoparticles as a novel carrier for the delivery of anthraquinone: Synthesis, characterization and in vitro cytotoxicity evaluation, Colloids Surf. B: Biointerface **101** (2013) 126-134.

29. Trang N. T. T., Chinh N. T., Mai T. T., Trung T. H., Hoang T. - Investigation of effect of polyethylene oxide on properties and morphology of polylactic acid/chitosan/quinine composites, Vietnam J. Chem. **57** (1) (2019) 52-56.
30. Trang N. T. T., Mai T. T., Trung T. H., Cong D. V., Lam T. D., Hoang T. - Study on characteristic, properties and morphology of poly(lactic acid)/chitosan/hydroquinine green nanoparticles, Green Process. Synth. **7** (5) (2018) 417-423. https://doi.org/10.1515/gps-2018-0025.
31. Rajan M., Raj V. - Formation and characterization of chitosan-polylacticacid-polyethylene glycol-gelatin nanoparticles: A novel biosystem for controlled drug delivery, Carbohydr. Polym. **98** (2013) 951-958.
32. Thapa C., Jo-Eun S., Taekwang K., Gyubin N., Santosh B., Shrawani L., Jung H. K., Jae H. L., Jee H. P., Jaewoong C., *et al*. - Optimized self-microemulsifying drug delivery system improves the oral bioavailability and brain delivery of coenzyme Q10, Drug Deliv. **29** (1) (2022) 2330-2342, DOI: 10.1080/10717544.2022.2100515
33. Ashok K. J., Tahani I., Kai B. L., Manogaran E., Hanish S. J. C. - Improved oral bioavailability of poorly water-soluble vorinostat by self-microemulsifying drug delivery system, Beni-Suef University J. Basic Appl. Sci. **11** (2022) 99.
34. Trang T. D. M., Chinh N. T., Tham D. Q., Giang B. L., Nghia T. H., Trung V. Q., Hoang T. - Preparation and characterization of chitosan/fish scale collagen/lovastatin nanocomposites, J. Polym. Environ. **28** (11) (2020) 2851-2863. DOI 10.1007/s10924-020-01819-3
35. Alshahrani S. M., Alshetaili A. S., Alalaiwe A., Alsulays B. B., Answer M. K., Al-Shdefat R., Imam F., Shakeel F. - Anticancer efficacy of self-nanoemulsifying drug delivery system of sunitinib malate, AAPS Pharm. Sci. Tech. **19** (2018) 123-133.
36. Yeeun L., Donghyun L., Eunyoung P., Seok-Young J., Seo Y. C., Seongryeong H., and Heebeom K. - Rhamnolipid-coated W/O/W double emulsion nanoparticles for efficient delivery of doxorubicin/erlotinib and combination chemotherapy, J. Nanobiotechnol., **19** (2021) 411. https://doi.org/10.1186/s12951-021-01160-4
37. Eliana B. S., Amanda C., Carlos M. G., Tiago E. C., Aleksandra Z. and Amélia M. S. - Microemulsions and nanoemulsions in skin drug delivery, Bioengineering **9** (4) (2022) 158. https://doi.org/10.3390/bioengineering9040158
38. Cerqueira-Coutinho C., Santos-Oliveira R., dos Santos E., Mansur C. R. - Development of a photoprotective and antioxidant nanoemulsion containing chitosan as an agent for improving skin retention, Eng. Life Sci. **15** (2015) 593-604.
39. Sharma B., Iqbal B., Kumar S., Ali J., Baboota S. - Resveratrol-loaded nanoemulsion gel system to ameliorate UV-induced oxidative skin damage: From in vitro to in vivo investigation of antioxidant activity enhancement, Arch. Dermatol. Res. **311** (2019) 773-793.
40. Gupta R., Shea J., Scaife C., Shurlygina A., Rapoport N. - Polymeric micelles and nanoemulsions as drug carriers: Therapeutic efficacy, toxicity, and drug resistance, J. Control. Release **212** (2015) 70-77.
41. Haggag Y. A., Faheem A. M., Tambuwala M. M., Osman M. A., El-Gizawy S. A., O'Hagan B., Irwin N., McCarron P. A. - Effect of poly(ethylene glycol) content and formulation parameters on particulate properties and intraperitoneal delivery of insulin

from PLGA nanoparticles prepared using the double-emulsion evaporation procedure, Pharm. Develop. Technol. **23** (2018) 370-381. https://doi.org/10.1080/10837450.2017.1295066

42. Chaudhary S., Aqil M., Sultana Y., Kalamk M. A. - Self-nanoemulsifying drug delivery system of nabumetone improved its oral bioavailability and anti-inflammatory effects in rat model, J. Drug Delivery Sci. Technol. **51** (2019) 736-745. https://doi.org/10.1016/j.jddst.2018.04.009
43. Echeverri J. D., Alhajj M. J., Montero N., Yarce C. J., Barrera-Ocampo A., Salamanca C. H. - Study of in vitro and in vivo carbamazepine release from coarse and nanometric pharmaceutical emulsions obtained via ultra-high-pressure homogenization, Pharmaceuticals **13** (2020) 53. doi: 10.3390/ph13040053.
44. Laxmi M., Bhardwaj A., Mehta S., Mehta A. - Development and characterization of nanoemulsion as carrier for the enhancement of bioavailability of artemether, Artif. Cells Nanomed. Biotechnol. **43** (2015) 334-344. doi: 10.3109/21691401.2014.887018.
45. Rapoport N., Nam K. H., Gupta R., Gao Z., Mohan P., Payne A., Todd N., Liu X., Kim T., Shea J., et al. - Ultrasound-mediated tumor imaging and nanotherapy using drug loaded, block copolymer stabilized perfluorocarbon nanoemulsions, J. Control. Release **153** (2011) 4-15. https://doi.org/10.1016/j.jconrel.2011.01.022.